

Breakdown of the Endothelial Barrier Function in Tumor Cell Transmigration

Claudia Tanja Mierke,* Daniel Paranhos Zitterbart,* Philip Kollmannsberger,* Carina Raupach,* Ursula Schlötzer-Schrehardt,† Tamme Weyert Goecke,‡ Jürgen Behrens,§ and Ben Fabry*

*Biophysik, Zentrum für medizinische Physik und Technik, †Augenklinik, ‡Frauenklinik, §Nikolaus-Fiebiger Zentrum für Molekulare Medizin, Universität Erlangen-Nürnberg, 91052 Erlangen, Germany

ABSTRACT The ability of tumor cells to metastasize is associated with a poor prognosis for cancer. During the process of metastasis, tumor cells circulating in the blood or lymph vessels can adhere to, and potentially transmigrate through, the endothelium and invade the connective tissue. We studied the effectiveness of the endothelium as a barrier against the invasion of 51 tumor cell lines into a three-dimensional collagen matrix. Only nine tumor cell lines showed attenuated invasion in the presence of an endothelial cell monolayer, whereas 17 cell lines became invasive or showed a significantly increased invasion. Endothelial cells cocultured with invasive tumor cells increased chemokine gene expression of IL-8 and Gro- β . Expression of the IL-8 and Gro- β receptor, CXCR2, was upregulated in invasive tumor cells. Addition of IL-8 or Gro- β increased tumor cell invasiveness by more than twofold. Tumor cell variants selected for high CXCR2 expression were fourfold more invasive in the presence of an endothelial cell layer, whereas CXCR2 siRNA knock-down cells were fivefold less invasive. We demonstrate that Gro- β and IL-8 secreted by endothelial cells, together with CXCR2 receptor expression on invasive tumor cells, contribute to the breakdown of the endothelial barrier by enhancing tumor cell force generation and cytoskeletal remodeling dynamics.

INTRODUCTION

Most cancer-related deaths are caused by metastasis formation, a process that starts with dissociation of tumor cells from the primary tumor and is followed by tissue invasion, entrance into blood or lymph vessels (intravasation), and transport to remote sites. It is widely assumed that tumor cells can then escape from the microvasculature (extravasation), invade the target tissue, and form secondary tumors in distant organs (1–3). A potentially rate-limiting step in metastasis formation, therefore, would be the extravasation process that involves adhesion of tumor cells to endothelial cells and their transmigration through the endothelial cell monolayer and basement membrane (3–6). Certain tumor cell types have indeed been shown, both *in vitro* and *in vivo*, to be able to overcome the endothelial barrier (6–11). But extravasation need not be the only mechanism for metastasis formation, as has recently been pointed out by Al-Mehdi et al. (12), who reported that tumor cells can adhere and grow onto the endothelial layer and form a metastasis without ever leaving the blood or lymph vessel. Either way, the role of the endothelial monolayer in this process is thought to be crucial in that it can actively modulate metastasis formation by either allowing or block-

ing the adhesion, and possibly transmigration, of tumor cells (8–10). The details of endothelial cell functions in this process, however, are poorly understood, and the extent to which the endothelium impedes or promotes metastasis formation is still unclear.

Transmigrating tumor cells are thought to be able to overcome the endothelial barrier by inducing changes within endothelial cells, including the upregulation of adhesion molecule receptor expression (13), the reorganization of the cytoskeleton (14), Src-mediated disruption of endothelial VE-cadherin- β -catenin cell-cell adhesions (7), the formation of “holes” within the endothelial layer (15), and the induction of apoptosis (16). Tumor cell invasion may bear a close resemblance to leukocyte trafficking for which the endothelium acts as a barrier and greatly reduces invasion rates (17). For example, the function of the endothelial cell barrier against both leukocyte trafficking and tumor cell transmigration is reduced in the presence of inflammatory cytokines such as tumor necrosis factor- α and interleukin-1 β (8,13,18,19). These cytokines are known to trigger an upregulation of the adhesion molecule E-selectin (13). The subsequent adhesion of tumor cells to E-selectin leads to an upregulation of stress-activated protein kinase-2 (SAPK2/p38) in endothelial cells (13) and triggers actin polymerization and reorganization into stress fibers (14).

Chemokines and their receptors are also important for leukocyte trafficking (20,21) and tumor cell invasion (22). Chemokines are a superfamily of small cytokine-like proteins that induce cytoskeletal rearrangements in endothelial cells and leukocytes, the firm adhesion of leukocytes to endothelial cells, and the directional migration of leukocytes (20). The involvement of chemokines in tumor-endothelial interactions

Submitted June 11, 2007, and accepted for publication November 6, 2007.

Address reprint requests to Dr. Claudia Tanja Mierke, University of Erlangen-Nuremberg, Center for Medical Physics and Technology, Biophysics Group, Henkestrasse 91, 91052 Erlangen, Germany. Tel.: 49-9131-85-25607; Fax: 49-9131-85-25601; E-mail: claudia.mierke@t-online.de.

This is an Open Access article distributed under the terms of the Creative Commons-Attribution Noncommercial License (<http://creativecommons.org/licenses/by-nc/2.0/>), which permits unrestricted noncommercial use, distribution, and reproduction in any medium, provided the original work is properly cited.

Editor: Cristobal G. dos Remedios.

© 2008 by the Biophysical Society
0006-3495/08/04/2832/15 \$2.00

doi: 10.1529/biophysj.107.113613

and their effect on tumor cell mechanics during invasion are considerably less well understood, however.

The aim of this study was to investigate the ability of the endothelium to regulate the transmigration and invasion of tumor cells into an extracellular matrix. We measured the invasion of human tumor cell lines into a three-dimensional collagen gel matrix that was covered with an endothelial cell monolayer. In the presence of an endothelium, the invasion of some tumor cell lines increased significantly. Gene expression analysis of endothelial cells cocultured with invasive tumor cells revealed an upregulation of Gro- β and IL-8 chemokines compared with endothelial cells cocultured with noninvasive tumor cells. Finally, we demonstrate that the Gro- β and IL-8 receptor (CXCR2) expression on tumor cells serves as a key mediator responsible for the breakdown of the endothelial barrier function by enhancing tumor cell force generation and cytoskeletal remodeling dynamics.

MATERIALS AND METHODS

Three-dimensional collagen assay

All chemicals were purchased from Sigma (Taufkirchen, Germany) unless otherwise noted. Collagen R (Serva, Heidelberg, Germany) and G (Biochrom, Berlin, Germany) were mixed at a ratio 1:1, 25 mM sodium bicarbonate and 10 vol % of 10 \times DME (Biochrom) was added. The solution was neutralized with 1 N sodium hydroxide, and 1.2 ml collagen solution was placed into each well of a six-well plate, polymerized, incubated with Endothelial Cell Growth Medium 2 (Promocell, Heidelberg, Germany) containing 2% low-endotoxin FCS, and 600,000 endothelial cells (first passage) were seeded onto the gel. Polymerized collagen gels were 474 $\mu\text{m} \pm 7$ (mean \pm SE, $n = 12$) thick. After 24 h, the cells had formed a closed monolayer, and 100,000 tumor cells were added per 3.5-cm dish. To study invasion in the absence of endothelial cells, tumor cells were added directly to the gels. Before seeding, tumor cells were stained with 5 $\mu\text{g}/\text{ml}$ carboxyfluorescein diacetate (Invitrogen, Karlsruhe, Germany) and 1 $\mu\text{g}/\text{ml}$ Hoechst 33342 dye to distinguish them from endothelial cells. Coculture times ranging from 8 h to 5 d were tested. Staining was stable over the course of the experiment; the Hoechst dye was found to exhibit only insignificant photobleaching, and the carboxyfluorescein diacetate, although it was prone to photobleaching, was adequate for confirming that endothelial cells did not invade the collagen matrix. A coculture time of 72 h was found to be optimal because differences in the invasiveness of tumor cell lines were clearly visible while the endothelial monolayer was still confluent, with no signs of tube formation or invasion. After fixation with 2.5% glutaraldehyde solution, the number of invaded tumor cells and their invasion depth were determined in 12 randomly selected fields of view. Invasion depth was determined by focusing the microscope on the center of the nucleus; the value was read from the motorized z -drive of the microscope and was corrected for the refractive index of water (1.33). The z -focus at the gel surface was taken as reference. Images were taken using a CCD camera (ORCA ER, Hamamatsu, DMI6000 Leica microscope, Wetzlar, Germany, 40 \times HCX fluotar objective, NA 0.6, Wasabi software).

Cell isolation and culture

Endothelial cells were isolated from the veins of human umbilical cords (HUVECs) (23). The vein was washed with PBS buffer, and endothelial cells were isolated using trypsin/EDTA solution (0.25%/0.2%) in PBS for 20 min at 37°C. HUVECs were maintained in endothelial medium (see above). HUVEC purity was determined by FACS analysis using VE-cadherin (Coulter, Krefeld, Germany) and PECAM-1 (Biozol, Eching, Germany). Iso-

lations contained less than 0.3% contaminating cells. Human pulmonary endothelial cells (HPMECs, Promocell) were used in passage 4–6 and cultured in Endothelial Cell Growth Medium MV 2 (Promocell) containing 5% FCS.

Tumor cells (ATCC-LGC-Promochem, Wesel, Germany) were cultured in DMEM (containing 1g/liter D-glucose, 10% low endotoxin FCS, 100 U/ml penicillin, 100 $\mu\text{g}/\text{ml}$ streptomycin) to 80% confluency and used in passages 5 to 30. All cells were cultured at 37°C, 95% humidity, and 5% CO₂, harvested using Accutase (PAA, Linz, Austria) and tested for mycoplasma contamination using a Mycoplasma-Detection-Kit (Roche, Penzberg, Germany). Primary tumor cells were isolated from kidney clear cell carcinomas using collagenase D and were used in passages 3–10. Primary tumor cells expressed E-cadherin (Coulter) and MUC-18 (Coulter) and did not express PECAM-1 or VE-Cadherin.

Transmission EM

Cells were fixed in 4% paraformaldehyde/0.1% glutaraldehyde in 0.1 M phosphate buffer, postfixed in 2% buffered osmium tetroxide, dehydrated through a graded ethanol series and embedded in epoxy resin. The 1.0- μm sections for orientation were stained with toluidine blue. Ultrathin sections (70 nm) were stained with uranyl acetate and lead citrate and examined with a transmission electron microscope (EM906E; Zeiss, Oberkochen, Germany).

Scanning EM

Fixed cells and gels were dehydrated through a graded ethanol series, washed with hexadimethylsilazane reagent (Electron-Microscopy-Science, Hatfield, PA), and air-dried. Cells were sputter-coated with gold and analyzed using a scanning electron microscope (ISI-SX-40, International Scientific Instruments, Milpitas, CA).

Cell sorting for gene expression analysis

Carboxyfluorescein-diacetate-stained tumor cells were cultured onto a HUVEC monolayer for 16 h. Cells were harvested, stained with a mouse anti PECAM-1 antibody and a secondary R-PE-labeled anti mouse IgG (F(ab)₂ fragment) antibody (Dianova, Hamburg, Germany) to detect endothelial cells, and separated using a cell sorter (Moflow, DakoCytomation). The purity of sorted endothelial cells and tumor cells was better than 99%.

RNA isolation and DNA microarray hybridization

After cell sorting, endothelial cells from mono- or coculture with MDA-MB-231, 786-O, MCF-7, and SW480 tumor cells were centrifuged (250 \times g, 5 min, 4°C). The pellet was resuspended in Trizol reagent (5 min, RT, Invitrogen), and total RNA was isolated according to the manufacturer's instructions. RNA was digested with RNase-free DNase I and purified using the RNeasyKit (Qiagen, Hilden, Germany) according to the manufacturer's instructions. RNA quality was checked by gel electrophoresis and spectrophotometric measurement of OD at 260/280 nm. cDNA synthesis and synthesis of biotinylated cRNA were performed as described by Thomas et al. (24). Human genome HG-U133A GeneChips (containing 22,283 open reading frames/genes, Affymetrix, Santa Clara, CA) were hybridized, washed, and scanned with the G2500A GeneArray scanner (Affymetrix) in cooperation with Dr. Möröy and Dr. Klein-Hitpass, Institute of Cell Biology (Tumor Research), University of Essen Medical School.

DNA-Microarray data analysis

Microarray data were analyzed using MicroarraySuite 5.1 and DataMiningTool 3.0 (Affymetrix). Gene expression levels of cocultured endothelial cells were normalized by the expression levels of monocultured cells

(same isolation). Mono- and cocultured endothelial cells were stained and sorted equally to eliminate bias. Statistical analyses were performed using Student's *t*-test. The expression of a HUVEC gene was considered to be correlated with tumor invasiveness when the following criteria were met: the expression level was higher than 500 Affymetrix units in at least one of the culture conditions (the median expression level of all genes was 273 Affymetrix units); the expression level after coculture with invasive versus non-invasive tumor cells was at least 1.8-fold different; and the expression levels of that gene did not overlap between noninvasive and invasive coculture conditions. Genes expressed in tumor cells at levels higher than 5000 Affymetrix units were disregarded to avoid contamination artifacts. We confirmed the microarray data for IL-8, Gro- β , ICAM-1, and VCAM-1 using RT-PCR.

Flow cytometry

Tumor cells were harvested and resuspended in Hepes buffer (20 mM Hepes, 125 mM NaCl, 45 mM glucose, 5 mM KCl, 0.1% albumin, pH 7.4). Cells were incubated with mouse antibodies directed against CXCR1, CXCR2, CXCR3, CCR2 (all R&D systems, Minneapolis, MN), or CXCR4 (Dianova). Appropriate isotype controls (mouse IgG₁, IgG_{2a}, and IgG_{2b}) were used (Invitrogen). After 30 min of incubation at 4°C, the cells were washed and stained with a secondary R-PE-labeled anti-mouse IgG antibody. FACS analysis was performed using a FACSCalibur system (Becton Dickinson, Heidelberg, Germany).

Isolation of tumor cell variants

For the isolation of tumor cell variants expressing low and high amounts of CXCR2, tumor cells were stained as described above under flow cytometry. Low and high CXCR2-expressing tumor cell variants were separated using a cell sorter. Cells were expanded in culture, and the isolation and sorting procedures were repeated three times.

siRNA transfection

A quantity of 200,000 MDA-MB-231 cells were seeded into each six-well plate. Ten minutes later, a transfection mixture containing 2.4 μ l of a 20 μ M Alexafluor546-labeled CXCR2 RNAi solution (target-sequence AGGATTTAAGTTTACCTCAAA) and 12 μ l HiPerFect Reagent (Qiagen) in 100 μ l DMEM, was added and incubated at room temperature for 10 min. RNAi-mediated CXCR2-knockdown and transfection efficiency were determined by FACS-analysis using an anti-CXCR2 antibody and a Cy2-labeled anti-mouse antibody (Dianova).

CXCR2 inhibition

CXCR2 inhibitor SB255002 (Calbiochem, San Diego, CA) was added together with tumor cells (100,000 per six-well plate) at concentrations ranging from 2.2 nM to 28.4 μ M. Invasiveness was determined after 3 days of coculture.

Cell mechanics

For creep measurements, a staircase-like sequence of step forces ranging from 0.5 to 10 nN was applied to superparamagnetic 4.5- μ m epoxytated, fibronectin-coated beads (Invitrogen) using magnetic-tweezers as described by Alenghat et al. (25) and Mierke et al. (26). After 30 min of bead incubation, measurements were performed at 37°C on an inverted microscope (DMI Leica) with 40 \times magnification using monocultured MDA-MB-231 wild type and CXCR2 siRNA knockdown cells. Bright-field images were taken by a CCD camera (ORCA ER) at 40 frames/s. The bead positions were tracked using an intensity-weighted center-of-mass algorithm (27). The creep

response $J(t)$ of the cells followed a power law in time, $J(t) = a(t/t_0)^b$, where the prefactor a and the power-law exponent b were both force dependent, and the reference time t_0 was set to 1 s. The bead displacement in response to a staircase-like force followed a superposition of power laws (28) (see Fig. 7 A), from which the power-law exponent b was determined by a least-squares fit. In addition, the position of unforced beads was tracked over 5 min. These beads moved spontaneously with a mean-square displacement (MSD) that also followed a power law in time, $MSD = D^*(\Delta t/t_0)^\alpha + c$ using low and high CXCR2-expressing tumor cell variants (see Fig. 7 B). The power-law exponent α was determined by a least-squares fit (29,30). Cell tractions (see Fig. 7, C and D) were computed from the deformation field of an elastic fibronectin-coated (50 μ m/ml) 6-kPa polyacrylamide gel during cell adhesion using low and high CXCR2-expressing tumor cell variants (26,31).

Statistics

Data were expressed as mean values \pm SE if not indicated otherwise. Statistical analysis was performed using the two-tailed paired *t*-test. A $p < 0.05$ was considered to be statistically significant.

Online supplementary material

Table S1 shows all genes up- or downregulated in endothelial cells after coculture with invasive compared with noninvasive tumor cells. Fig. S2 shows the effect of CXCR2 (mean \pm SE) antagonist SB222005 on tumor cell transmigration; * $p < 0.05$.

RESULTS

Overcoming the endothelial barrier

To study tumor-transendothelial migration and tissue invasion, a three-dimensional collagen assay was developed (Fig. 1 A). Freshly isolated HUVECs were cultured onto a collagen gel and formed a confluent monolayer within 24 h (Fig. 1 B). Adjacent endothelial cells overlapped by ~ 2 μ m (Fig. 1 B inset). Collagen fibers formed a mesh with an average pore size of 0.6 ± 0.2 μ m (mean \pm SE); the gels had a shear modulus of 58 Pa and a thickness of 474 ± 7 μ m (mean \pm SE) (Fig. 1 C).

With this assay, the transmigration and invasion behavior was tested for 51 tumor cell lines derived from a broad spectrum of tissues (Table 1). Before the tumor cells were added to the assay, they were fluorescently labeled with carboxyfluorescein diacetate (to distinguish them from endothelial cells, Fig. 1 F) and with Hoechst 33342 vital stain (for cell counting and quantification of the invasion depth). All tumor cells were able to attach to the endothelium or the collagen gel surface, even those that are unable to attach tightly to a pure plastic cell culture surface such as Colo201 and Colo205. After 3 days, the number of tumor cells that had transmigrated through the endothelium was counted, and their invasion depth was measured. All tumor cell lines that invaded into the collagen gel assumed an elongated, spindle-shaped morphology that was drastically different from the fibroblast-like morphology seen in a two-dimensional plastic cell culture flask (Fig. 1 D). Furthermore, tumor cells in the gels formed long filopodia (Fig. 1 E).

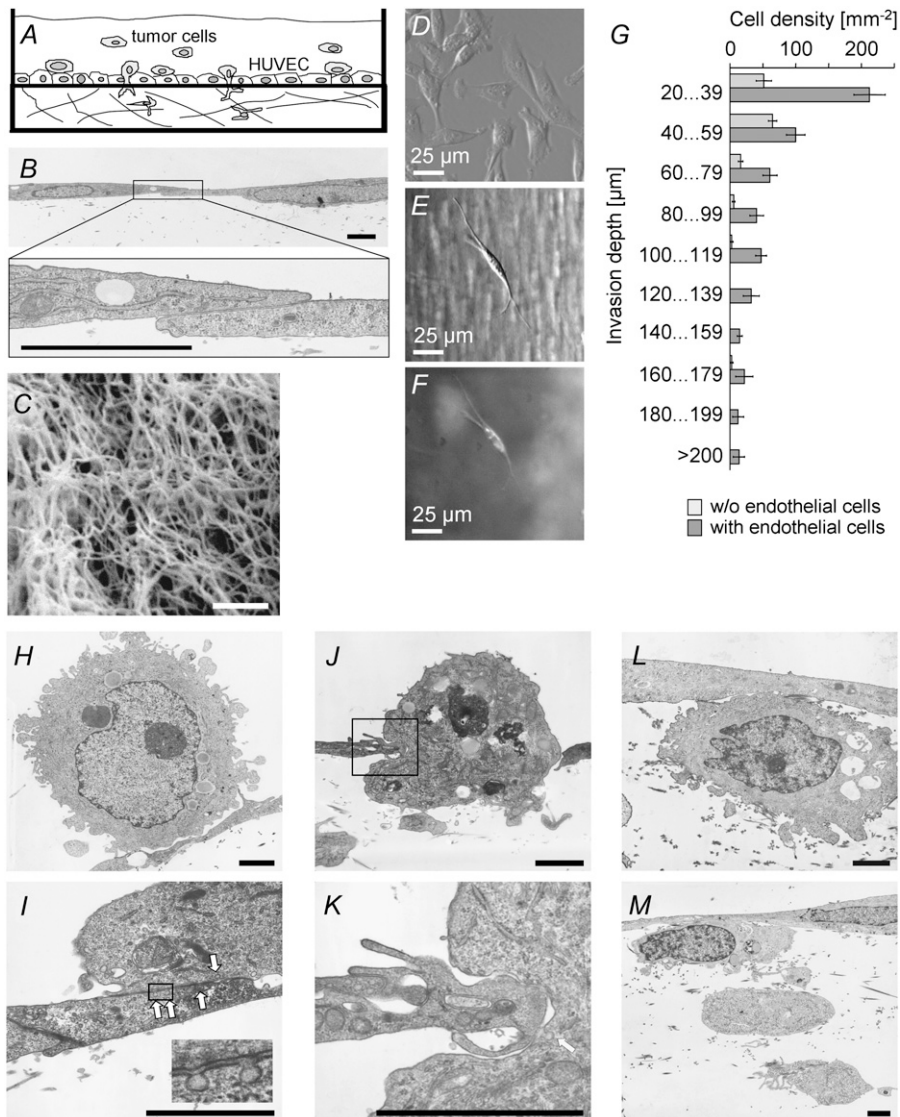


FIGURE 1 Transendothelial migration and collagen invasion of tumor cells. (A) Schematic diagram of the tumor cell transmigration and invasion assay. (B) TEM image of the endothelial cell monolayer. (C) SEM image of the three-dimensional collagen gel fiber network. (D and E) MDA-MB-231 breast carcinoma cells on plastic surface (D) showed an elongated spindle-shaped morphology in a three-dimensional collagen culture (E). (F) Same cell stained with carboxyfluorescein-diacetate. (G) The number of invaded MDA-MB-231 cells and their invasion depth were increased in the presence of an endothelium (dark gray) compared with endothelium-free culture (light gray). (H) Adhesion of an MDA-MB-231 cell and (I) of an SW480 cell onto the endothelium. Arrows indicate caveolae of tumor and endothelial cells. (J) Transmigration of an MDA-MB-231 cell through the endothelium. (K) An enlarged detail of the close contact between tumor and endothelial cells. (L) Invasion of an MDA-MB-231 cell, and (M) stack of three invaded MDA-MB-231 cells. Tumor cells transmigrated without destroying or disrupting the endothelium. Scale bars are $2 \mu\text{m}$ where unspecified.

As introduced above, several pathways of tumor cell transmigration are possible: disruption of cell-cell adhesion sites, “hole” formation, and induction of apoptosis in endothelial cells. To determine which pathway the tumor cells chose, we analyzed TEM sections of collagen gels taken after 4, 10, 16, and 24 h of tumor-endothelial cell coculture with noninvasive SW480 and MCF-7 tumor cells and with invasive MDA-MB 231, A125, 786-O, and A375 tumor cells. Fig. 1, H–M, illustrates the three steps of tumor cell extravasation: tumor cell adhesion (Fig. 1, H and I), transmigration (Fig. 1 J), and matrix invasion (Fig. 1 L and M). The adhesion process was completed after 4 h of coculture, and transmigration was detectable after 8 h. Among ~ 1000 analyzed TEM sections in which tumor cells were present, 20 tumor cells were in the process of transmigration, and ~ 100 cells had invaded into the collagen gel. For all transmigrating tumor cells, adjacent TEM sections were obtained to ensure

that endothelial cells were present on either side of the transmigrating tumor cell. This finding indicates that the tumor cells transmigrated not by “hole” formation but by disrupting the endothelial cell-cell contacts. Moreover, neighboring endothelial cells did not show morphological signs indicative of apoptosis such as membrane blebbing, cell shrinkage, or rounding. During tumor cell adhesion and transmigration, the contact regions of tumor and endothelial cells were decorated with multiple vacuoles and caveolae (Fig. 1, I and K, arrows). In all TEM sections of invaded tumor cells (Fig. 1, L and M), the endothelial monolayer completely resealed and appeared intact (Fig. 1, L and M). This was verified in multiple adjacent sections around each invaded tumor cell. We repeatedly found stacks of invaded tumor cells at different invasion depths at the same location (Fig. 1, L and M), suggesting that these tumor cells had used the same transmigration and invasion path.

Classification of tumor cell invasiveness

All cell lines were classified into invasive and noninvasive tumor cells according to their ability to invade the collagen gel. The invasion depth for all the tumor cells was measured in multiple randomly chosen fields of view. From the density (number of invaded cells per square millimeter) plotted against invasion depth, an invasion profile was obtained (Fig. 1 G). Invasiveness was quantified by an invasion score, defined as cell density multiplied by the average invasion depth. Tumor cell lines with an invasion score $\leq 0.1 \text{ mm}^{-1}$ were defined as noninvasive; a score $> 0.1 \text{ mm}^{-1}$ was defined as invasive. This threshold was chosen to avoid an erroneous classification of noninvasive cells. Twenty-four of 51 tumor cell lines were able to invade into the collagen gel when no endothelial cells were present (Table 1). All cell lines derived from skin (five lines), prostate (two), bladder (two), and kidney (two) were invasive; among cell lines derived from breast (14 lines), cervix (two), colon (16 lines), lung (four), and pancreas (two) were both invasive and noninvasive lines (Table 1).

Endothelial cells enhance tumor cell invasion

A conspicuous question is to what degree does the endothelial layer impede tumor cell invasion in a collagen matrix? In the presence of an endothelial monolayer, invasiveness was reduced in 9 of 24 invasive cell lines (Table 1), unchanged in 9 cell lines, and, surprisingly, significantly increased in 6 cell lines (Table 1). Eleven of 27 noninvasive tumor cell lines became weakly invasive in the presence of an endothelial layer (Table 1). We also studied primary tumor cells isolated from four patients with kidney clear cell carcinomas. In contrast to Caki-1 and 786-O kidney tumor cell lines, which did not alter their invasiveness, all four primary kidney carcinoma cells showed increased matrix invasion in the presence of an endothelium (data not shown).

The findings that the presence of the endothelium promoted invasion of some of the tumor cells and even induced invasion were unexpected and new. A possible interpretation of these results is that the endothelium promotes tumor cell proliferation. However, this interpretation is ruled out by the finding that the number of tumor cells after 16 h of monoculture compared with coculture on an endothelium was equal.

The collagen invasion assay was repeated in MDA-MB-231 tumor cells, but this time the endothelial layer was replaced by a closed monolayer of MCF-7 epithelial cells. MDA-MB-231 cell invasion was fully blocked by MCF-7 cells, indicating that the modulation of tumor cell invasion seen in our data was specific for the presence of endothelial cells. Experiments on all tumor cell lines were repeated with endothelial cells isolated from three to six different donors (250 in total) and were performed over 3 years with more than 10 batches of bovine and rat collagen. The standard deviation of the invasion scores within a tumor cell line was typically 30% of the mean, suggesting that effects of indi-

vidual HUVEC isolations or variations among collagen batches were minimal.

Both macrovascular and microvascular endothelial cells enhance tumor cell invasion

We replaced macrovascular HUVECs with primary HPMECs isolated from lung resections and analyzed 11 different tumor cell lines for their ability to overcome the endothelial cell barrier and to invade the three-dimensional collagen gels. In agreement with the data obtained with HUVECs, MCF-7, CX-1, Caco-2, and MDA-MB-468 cells remained completely noninvasive in the presence of a microvascular endothelial cell layer, the invasion of HeLa cells was significantly impeded, and the invasion of MDA-MB-231, T24, EJ-28, A375, and DU145 were significantly enhanced (Fig. 2). Note that the control experiments without endothelial cells were carried out in both HUVEC and HPMEC cell culture medium, which differ in their serum and hydrocortisone content, but the invasiveness of tumor cells was not markedly different. Interestingly, pulmonary microvascular ECs enhanced the invasion of MDA-MB-231 breast and T24 skin carcinoma cell to a markedly larger extent than HUVECs, and they induced the invasion of A431 lung carcinoma into the collagen matrix (Fig. 2). Despite these important differences, HUVECs provide an appropriate and convenient model system to study breakdown of the endothelial barrier function against tumor cell invasion.

Endothelial chemokines enhance transmigration and invasion of some tumor cells

Gene expression analysis of endothelial cells was performed to identify candidate genes responsible for the enhancement of tumor cell transmigration and invasion. The expression profile of endothelial cells in monoculture or after 16 h of coculture with tumor cells was analyzed using DNA microarrays. For coculture, two noninvasive cell lines (MCF-7 and SW480) and two invasive cell lines (MDA-MB-231 and EJ-28) were chosen. Our choice of MDA-MB-231 and EJ-28 cells was guided by their highly invasive behavior and their pronounced increase in invasiveness in the presence of an endothelium (Table 1).

Comparison of the gene expression profile under monoculture and coculture revealed 257 genes with expression levels that correlated with invasiveness (Fig. 3 and Table S1). Seventy-six genes were decreased, and 182 genes were increased in endothelial cells when cocultured with invasive tumor cells. Among the genes with increased expression were the chemokines Gro- β , IL-8, and I-TAC (Fig. 3 A). The expression of another chemokine, MCP-1, was increased in endothelial cells (by 6.5-fold) only during coculture with EJ-28 bladder carcinoma cells. Because MCP-1 has been described as enhancer for PC-3 prostate carcinoma cell invasiveness (32), it was included in a subsequent invasion

TABLE 1 Classification of tumor cell invasiveness

	Effect of HUVEC	Cell line	Tissue	Invasion score w/o HUVEC	Invasion score with HUVEC	
Noninvasive	Unchanged	Colo205	Colon	0.05 ± 0.02	0 ± 0	
		BT-20	Breast	0 ± 0	0 ± 0	
		Caco-2	Colon	0 ± 0	0 ± 0	
		CX1	Colon	0 ± 0	0 ± 0	
		KS	Breast	0 ± 0	0 ± 0	
		MDA-MB-453	Breast	0 ± 0	0 ± 0	
		MDA-MB-468	Breast	0 ± 0	0 ± 0	
		HCT116	Colon	0.01 ± 0.01	0.01 ± 0	
		MCF-7	Breast	0.08 ± 0.02	0.08 ± 0.02	
		CapanI	Colon	0 ± 0	0.01 ± 0.01	
		SW948	Colon	0 ± 0	0.01 ± 0.01	
		HS578T	Breast	0.04 ± 0.01	0.06 ± 0.01	
		A431	Lung	0 ± 0	0.02 ± 0.01	
		Colo201	Colon	0.03 ± 0.01	0.05 ± 0.01	
		A427	Lung	0 ± 0	0.37 ± 0.09	
		DLD-1	Colon	0.07 ± 0.02	0.14 ± 0.03	
		Induction of invasion	SW48	Colon	0 ± 0	0.05 ± 0.01
	CX-2		Colon	0 ± 0	0.06 ± 0.03	
	LX-1		Colon	0 ± 0	0.13 ± 0.03	
	T47D		Breast	0 ± 0	0.14 ± 0.03	
	HT-29		Colon	0 ± 0	0.15 ± 0.02	
	A549		Lung	0 ± 0	0.48 ± 0.09	
	SW620		Colon	0.01 ± 0	0.08 ± 0.02	
	SW480		Colon	0.02 ± 0.01	0.06 ± 0.02	
	MS751		Cervix	0.02 ± 0.01	0.07 ± 0.01	
	A172		Brain	0.02 ± 0.01	0.1 ± 0.01	
	Mia-Paca-II	Pancreas	0.04 ± 0.01	0.16 ± 0.03		
Invasive	Decreased invasion	BT549	Breast	5.69 ± 0.20	0.52 ± 0.10	
		MDA-MB-436	Breast	5.05 ± 0.60	0.96 ± 0.19	
		Mewo	Skin	3.04 ± 0.32	0.02 ± 0.01	
		PC-3	Prostate	6.13 ± 0.66	3.86 ± 0.4	
		SKBR3	Breast	3.02 ± 0.44	1.30 ± 0.13	
		Hacat	Colon	0.98 ± 0.18	0.04 ± 0.01	
		Hela	Skin	1.01 ± 0.10	0.34 ± 0.09	
		Me180	Cervix	1.38 ± 0.49	0.76 ± 0.20	
		DANG	Pancreas	0.86 ± 0.11	0.26 ± 0.03	
		Unchanged	C33A	Colon	0.53 ± 0.06	0.39 ± 0.08
			MDA-MB-361	Breast	0.24 ± 0.03	0.18 ± 0.02
			A875	Skin	0.35 ± 0.06	0.31 ± 0.05
			RT112	Bladder	0.32 ± 0.06	0.34 ± 0.07
	CAKI-1		Kidney	0.11 ± 0.03	0.21 ± 0.04	
	MDA-MB-435		Breast	1.09 ± 0.15	1.23 ± 0.2	
	786-0		Kidney	0.29 ± 0.04	0.59 ± 0.14	
	FaDu		Hypopharynx	0.65 ± 0.13	1.39 ± 0.28	
	A125		Lung	3.15 ± 0.29	3.38 ± 0.28	
	Increased invasion		A375	Skin	0.55 ± 0.09	2.49 ± 0.34
		DU145	Prostate	0.67 ± 0.05	2.89 ± 0.25	
		1205Lu	Breast	0.82 ± 0.20	1.52 ± 0.36	
		T24	Skin	2.04 ± 0.12	3.98 ± 0.51	
		MDA-MB-231	Breast	2.52 ± 0.12	8.05 ± 0.55	
		EJ-28	Bladder	3.84 ± 0.42	9.01 ± 1.00	

Invasion scores (mean ± SE) of 51 tumor cell lines cultured for 3 days on a three-dimensional collagen gel (100,000 tumor cells per 35 cm² dish) in the absence and presence of endothelial cells. An invasion score <0.1 was defined as noninvasive ($n = 27$), and an invasion score of >0.1 was defined as invasive ($n = 24$). In some tumor cell lines, the endothelium decreased transmigration and invasion ($n = 9$, for all $p < 0.05$), but in others, it significantly enhanced or induced transmigration and invasion (for all $p < 0.05$).

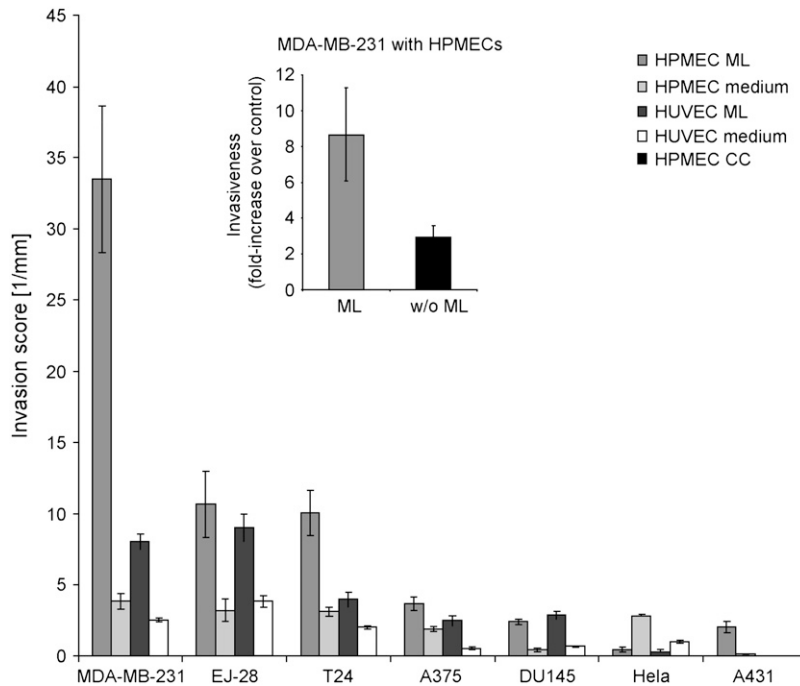


FIGURE 2 Microvascular and macrovascular endothelial cells enhanced tumor cell transmigration and invasion. Invasion score (mean \pm SE) of selected tumor cells in the presence and absence of a HPMEC or HUVEC monolayer (ML). Note that the HPMEC medium contained 5% FCS, and the HUVEC medium contained only 2% FCS. Accordingly, the endothelial cell-free controls were performed with 2% and 5% FCS. Independent of the endothelial cell type used, the invasion score of cocultured cells was significantly increased for MDA-MB-231, T24, EJ-28, A375, DU145, or in the case of HeLa significantly decreased ($p < 0.05$). For the A431 lung carcinoma cells, the HPMECs significantly induced the invasion score compared with HUVECs ($p < 0.05$). (*inset*) Invasiveness of MDA-MB-231 cells cultured in the presence of a HPMEC monolayer (ML) or cocultured with HPMECs that were seeded at the same with the tumor cells but did not form a monolayer (w/o ML). Numbers are expressed as fold increase of the invasion score compared with MDA-MB-231 in monoculture. HPMECs increased MDA-MB-231 cell invasion in both cases, but the effect of a monolayer was more pronounced.

assay, which was performed to determine whether tumor cell transmigration and invasion were altered by Gro- β , IL-8, I-TAC, and MCP-1 stimulation.

Gro- β and IL-8 addition to 786-O kidney carcinoma cells increased transmigration and invasion significantly (Fig. 3 B). The effect of Gro- β and IL-8 was particularly pronounced in the presence of an endothelial cell monolayer. The chemokine concentrations of 100 ng/ml for Gro- β , 25 ng/ml for IL-8, and 20 ng/ml for I-TAC and MCP-1 were chosen according to Lu et al. (32) and Youngs et al. (33); twofold higher concentrations were also tested, and in the case of Gro- β , 10-fold lower and higher concentrations as well, but no further increase of invasiveness was found. I-TAC or MCP-1 did not enhance tumor cell invasion (Fig. 3 B). Gro- β , IL-8, I-TAC, and MCP-1 stimulation of noninvasive MDA-MB-468 breast carcinoma cells had no effect (data not shown). The morphology of tumor cells or HUVECs was not altered after chemokine stimulation (Fig. 3 C).

To distinguish between the potentially invasiveness-enhancing effect of chemokine secretion by the endothelial cells and the physical barrier function of a closed endothelial monolayer, we co-plated MDA-MB-231 breast carcinoma cells with microvascular endothelial cells that were both added onto native collagen gels at the same time. After 3 days of coculture, the presence of endothelial cells increased MDA-MB-231 cell invasion by threefold (Fig. 2, *inset*). This increase, however, was less pronounced than the ninefold increase of invasiveness seen in the case where an endothelial monolayer had already formed before the addition of tumor cells (Fig. 2, *inset*). This result points to a complete breakdown of the endothelial barrier function against the invasion of MDA-MB-231 cells, although it remains an open question

why endothelial cells in a monolayer can promote tumor cell invasion to a higher degree than an equal number of endothelial cells that have not yet formed a monolayer.

CXCR2 expression on tumor cells increases transmigration and invasion

The diverse effects of those chemokines suggest that invasive and noninvasive tumor cells express the chemokine receptors at different levels. The expression levels of the following chemokine receptors were analyzed for all 51 tumor cell lines: CXCR1 (IL-8 receptor), CXCR2 (IL-8 and Gro- β receptor), CXCR3 (I-TAC receptor), and CCR2 (MCP-1 receptor). For example, the histograms show the expression levels of the invasive MDA-MB-231 breast carcinoma cells and the noninvasive MCF-7 breast carcinoma cells (Fig. 4, A and B).

In addition, the expression level of the CXCR4 receptor was studied because CXCR4 has been reported to correlate with metastasis formation (34). FACS analysis on all 51 tumor cell lines showed that CXCR2 receptor expression (mean values averaged over 24 invasive cell lines and over 27 noninvasive tumor cell lines) was increased by 2.3-fold in invasive compared with noninvasive tumor cells (Figs. 4 D). All 24 invasive tumor cell lines expressed the CXCR2 receptor, although the expression level in A875 melanoma cells was low. The other receptors tested did not correlate with invasiveness (Fig. 4 D). Expression of CXCR1, CXCR2, or CXCR3 on freshly isolated HUVECs was low; expression of CXCR4 and CCR2 was detectable (Fig. 4 C). In agreement with the literature, expression levels of CXCR2 increased in higher passages of some endothelial cell isolations (35,36). To rule out that CXCR2 autocrine stimulation of endothelial

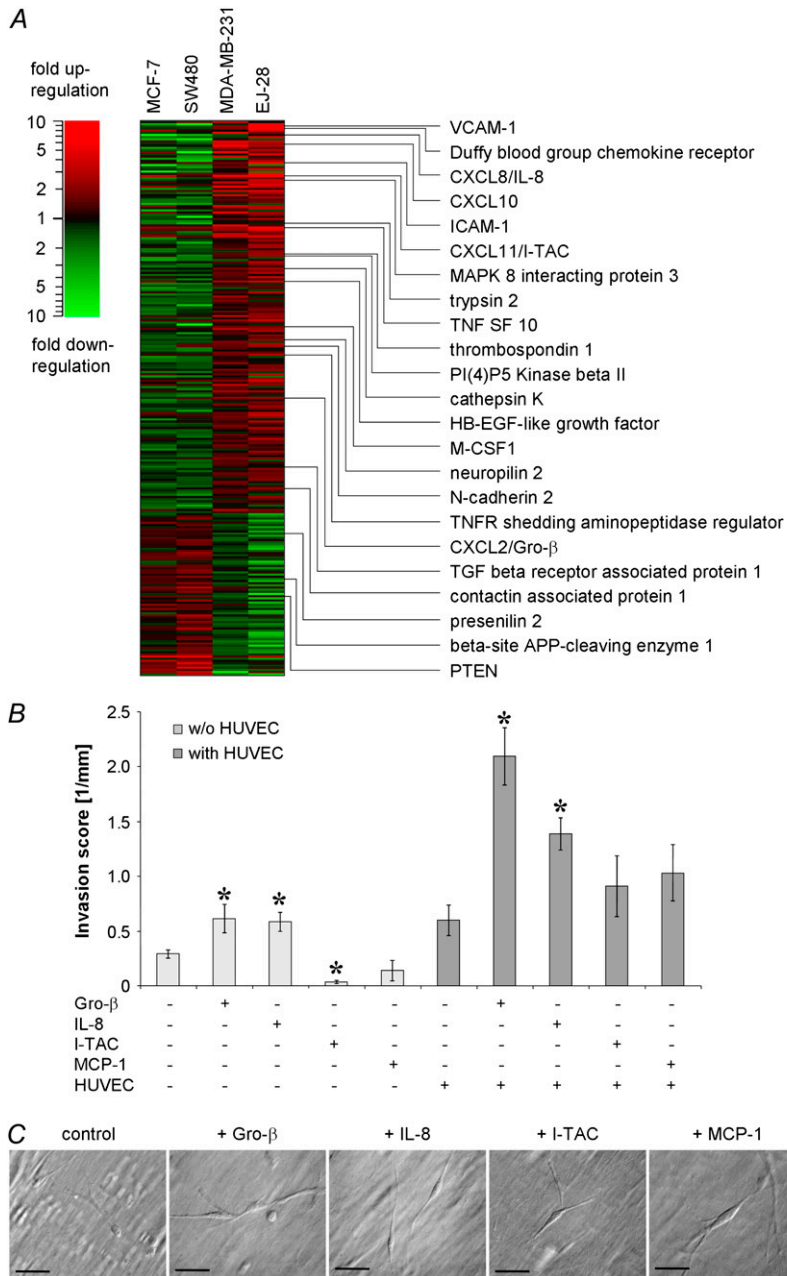


FIGURE 3 Chemokines enhanced tumor cell transmigration and invasion. (A) Expression profiles of genes that were upregulated (*red*) or downregulated (*green*) in endothelial cells cocultured with two invasive and two noninvasive tumor cells. Among the 257 regulated genes were numerous cytoskeletal proteins, adhesion molecules, and cytokines/chemokines. (B) Addition of the chemokines Gro- β (100 ng/ml) and IL-8 (25 ng/ml) significantly increased the invasion score (mean \pm SE, $*p < 0.05$) of 786-O kidney carcinoma cells both in the presence (*dark gray*) and absence of endothelial cells (*light gray*). No significant increase of invasiveness was seen after addition of the chemokines I-TAC (20 ng/ml) and MCP-1 (20 ng/ml). (C) Modulation contrast image of 786-O kidney carcinoma cells (invasion depth 50 μ m) show similar morphology under control conditions and under chemokine stimulation. Scale bars are 50 μ m.

cells affected the transmigration and invasion assays, only freshly isolated cells were used, and the CXCR2 expression levels of each endothelial cell isolation were determined.

To analyze the role of CXCR2 in the transmigration and invasion process, variants of invasive cell lines were isolated that expressed low and high amounts of CXCR2. Variants from the following tumor cell lines were generated using cell sorting after staining with an anti-CXCR2 antibody (numbers in parentheses give the CXCR2 expression ratio of the high/low variant): MDA-MB-231 (breast, 5.3), 786-O (kidney, 12.3), and DU145 (prostate, 4.0) (Fig. 5, A–C).

The transmigration and invasion behaviors of low and high CXCR2-expressing variants were analyzed in the three-

dimensional collagen assay in the absence or presence of an endothelial monolayer. Invasiveness of the CXCR2-high MDA-MB-231 variant was increased by twofold in the absence of endothelial cells, and increased by threefold in the presence of endothelial cells (Fig. 5 G). Invasiveness of the CXCR2-high 786-O variant was marginally increased in the absence of endothelial cells but increased by fourfold in the presence of endothelial cells (Fig. 5 H). Invasiveness of the CXCR2-high DU145 variant was marginally increased in the absence of endothelial cells but increased by fourfold in the presence of endothelial cells (Fig. 5 I).

To verify that tumor cell transendothelial migration and invasion were enhanced by high expression levels of CXCR2,

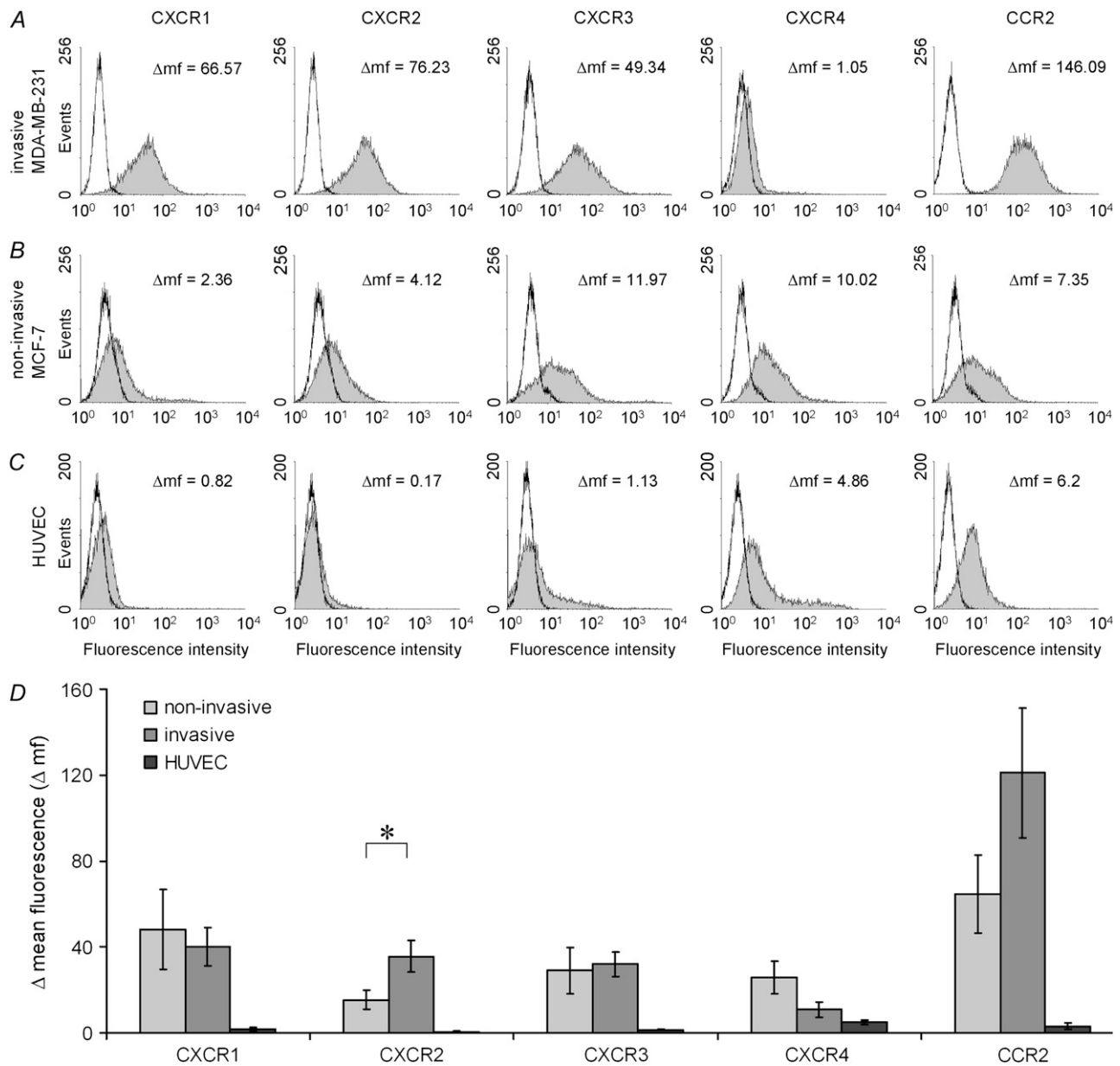


FIGURE 4 Chemokine receptor expression on tumor and endothelial cells. (A) Chemokine receptor expression on invasive MDA-MB-231 breast carcinoma cells, (B) noninvasive MCF-7 breast carcinoma cells, and (C) freshly isolated HUVECs in passage 0 were measured using FACS analysis. (D) Chemokine receptor expression (mean \pm SE) on invasive (dark gray, $n = 24$), and noninvasive tumor cells (light gray, $n = 27$) and HUVECs (black, $n = 3$ different isolations). Invasive tumor cells expressed 2.3-fold higher levels of CXCR2 compared with noninvasive tumor cells ($*p < 0.05$).

an RNAi-mediated transient knock-down of CXCR2 was performed in MDA-MB-231 cells using fluorescently labeled CXCR2 siRNA. The transfection efficiency was 99.2% as analyzed by counting transfected and nontransfected cells and by FACS analysis (Fig. 6, A, D, and E). CXCR2 receptor expression after siRNA knock-down was not detectable by FACS analysis (Fig. 6, B and C). Also, the cell morphology was not altered by CXCR2 siRNA transfection (Fig. 6, G–J). In the absence of an endothelial monolayer, the invasion of the CXCR2 knock-down cells was not reduced significantly, but importantly, the endothelium failed

to increase the invasiveness in these cells (Fig. 6 F). This result is consistent with the observation that the CXCR2 inhibitor SB225002 (28.4 μ M) completely blocked trans-endothelial migration and invasion of MDA-MB-231 cells (Fig. S2).

Chemokine-CXCR2 interactions increase tumor cell invasion by enhancing cytoskeletal dynamics and cell tractions

CXC receptor-ligand interactions can initiate a large number of signal transduction pathways that could contribute to

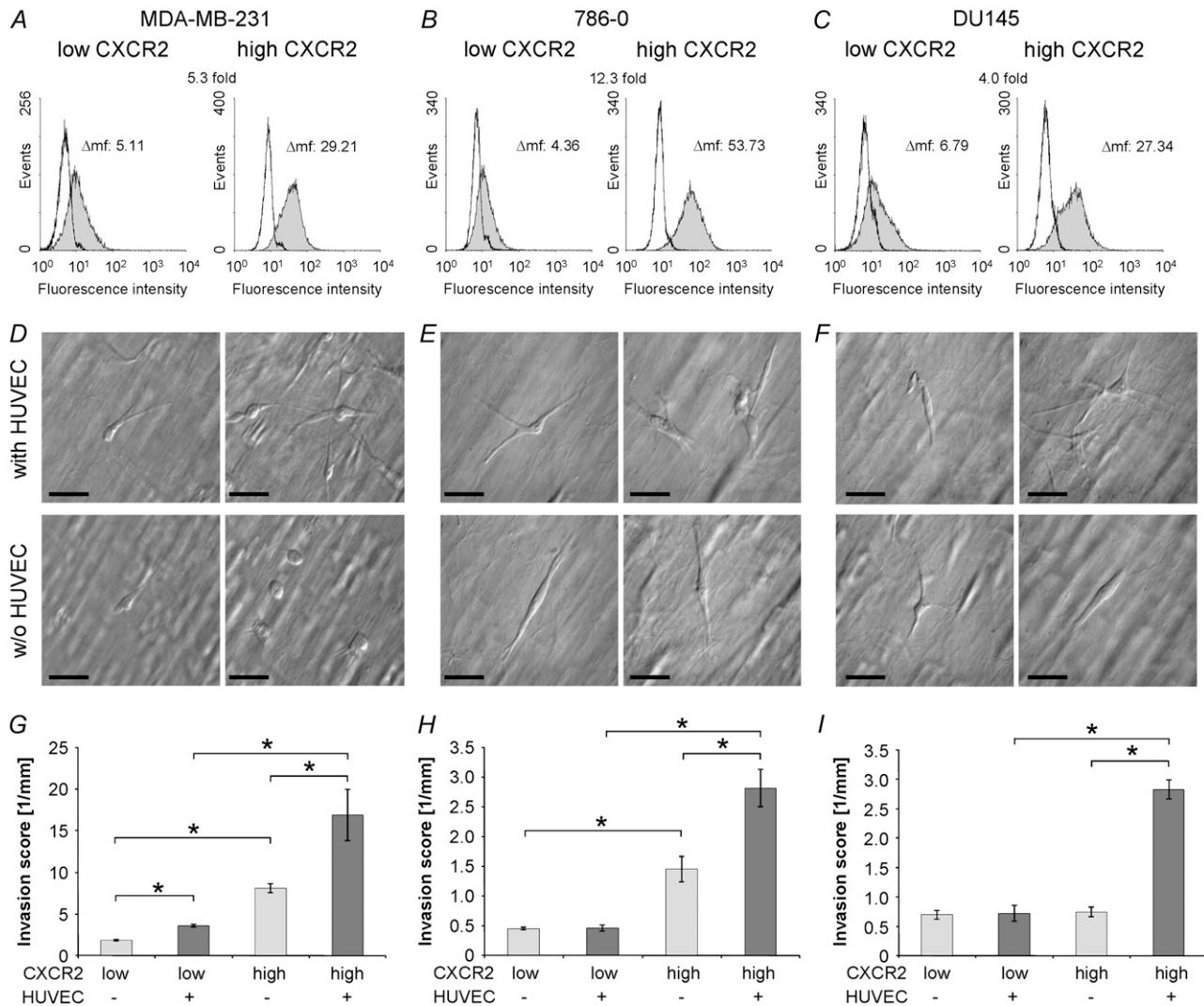


FIGURE 5 Analysis of CXCR2-low and CXCR2-high carcinoma cell variants. CXCR2 expression of CXCR2-low and CXCR2-high variants in (A) MDA-MB-231 breast, (B) 786-O kidney, and (C) DU145 prostate carcinoma cells after four cycles of sorting and subsequent culturing. In each histogram, left curves are isotype controls, and filled gray curves are CXCR2 expression on tumor cells. (D–I) Transmigration and invasion of MDA-MB-231 (left), 786-O (middle), and DU145 (right) variants expressing low and high amounts of CXCR2. (D–F) Modulation contrast images of CXCR2-low variants (left) and CXCR2-high variants (right) in a collagen gel (50–80 μm depths) in the absence (bottom) or presence (top) of an endothelial cell monolayer. Scale bars are 50 μm . (G–I) Invasion scores (mean \pm SE) of CXCR2-low and -high variants in the presence (dark gray bars) or absence of an endothelial cell monolayer (light gray bars). In the presence of a HUVEC monolayer, all CXCR2-high variants are significantly more invasive than CXCR2-low variants ($*p < 0.05$).

invasive and motile behavior of tumor cells by increasing actomyosin motor activity, adhesion/de-adhesion, and cytoskeletal remodeling events (37). The role of CXCR2 was explored using three cell-mechanical assays. The first was measuring the creep response of integrin-bound fibronectin-coated magnetic beads to step forces between 0.5 nN and 10 nN (Fig. 7 A). The creep response for all forces followed a power law over time. The exponent of the power-law creep response is a measure of bond stability. Exponents close to zero indicate stable bonds that result in an elastic, solid-like cell-mechanical behavior. Exponents close to unity indicate unstable bonds with high cycling or turnover rates that result in a viscous, fluid-like cell-mechanical behavior (27). In

MDA-MB-231 wild-type cells, the power-law creep exponent was significantly higher, closer to a fluid-like behavior, than in CXCR2 knock-down cells.

In the second assay, the random walk of unforced, spontaneously diffusing fibronectin-coated beads was analyzed (Fig. 7 B). These beads cannot move unless the microstructure to which they are attached rearranges (29). ATP-driven cytoskeletal rearrangements can be quantified by the superdiffusive power-law exponent of the MSD of the bead (29,30). The power-law exponent of the MSD in CXCR2-high cell variants was significantly more superdiffusive (Fig. 7 B), indicative of a higher rate of ATP-driven cytoskeletal rearrangements.

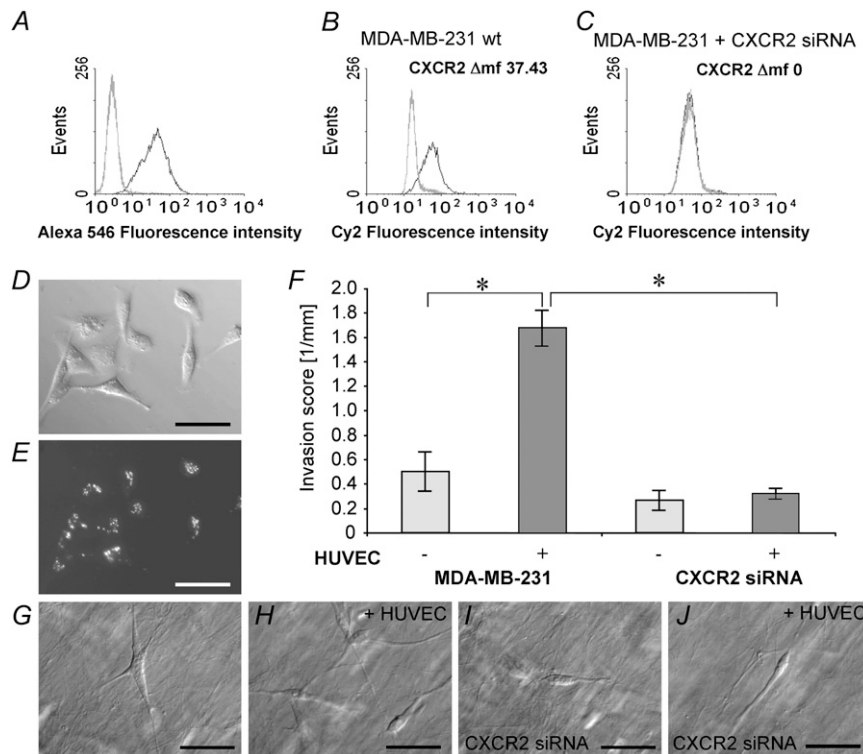


FIGURE 6 CXCR2 siRNA mediated knock-down significantly reduced tumor cell transendothelial migration and invasion. (A) FACS analysis of transfection efficiency. MDA-MB-231 breast carcinoma cells were transfected with CXCR2 siRNA fluorescently labeled with Alexa 546 (dark gray) and compared with nontransfected cells (light gray). (B) FACS analysis of CXCR2 expression levels in MDA-MB-231 control cells and (C) of cells transiently transfected with CXCR2 siRNA. (D) Modulation contrast image and (E) fluorescence image of MDA-MB-231 cells transiently transfected with CXCR2 siRNA. (F) In the presence of endothelial cells (dark gray bars), CXCR2 knock-down in MDA-MB-231 cells showed significantly reduced invasiveness ($*p < 0.05$). (G–J) Modulation contrast image of non-transfected MDA-MB-231 cells (G and H) and CXCR2 siRNA-transfected MDA-MB-231 cells in a collagen gel (50 μm depth) in the absence (H and J) or presence (G and I) of an endothelial cell monolayer. Scale bars are 50 μm .

The third assay explored actomyosin motor activity of MDA-MB-231 cells that expressed low or high amounts of CXCR2 using traction microscopy (31). In both variant cell lines, the tractions increased steadily on seeding during adhesion on an elastic fibronectin-coated polyacrylamide matrix. The strain energy and the tractions generated by CXCR2-high cells were eightfold higher than those generated by CXCR2-low cells (Fig. 7, C and D). Taken together, the mechanical effects of increased CXCR2 expression, such as increased cytoskeletal remodeling dynamics and force-generating capability, provide a plausible mechanism for the more invasive behavior seen in these tumor cells.

DISCUSSION

We developed a simple and reproducible assay consisting of a collagen matrix covered with an endothelial cell monolayer and measured the ability of 51 tumor cell lines derived from different tissues to transmigrate through the endothelium and invade the matrix (Fig. 1). Twenty-four cell lines were able to invade the collagen when an endothelial monolayer was absent (Table 1). To quantify and compare the invasiveness of the cell lines, an invasion score was used, which was computed as tumor cell density per square millimeter multiplied by the average invasion depth. The invasion scores presented here are consistent with the invasiveness of some of the cell lines previously tested by others (34,38).

To compare the invasiveness of tumor cell lines in the absence and presence of endothelial cells, collagen gels for

both conditions were prepared at the same time and with the same collagen batch. Type I collagen is the most abundant matrix protein in connective tissue: it is easy to polymerize and forms a fiber network structure with a defined pore size and reproducible mechanical properties (Fig. 1). However, for reasons of simplicity and reproducibility, this assay was limited in several ways. First, the collagen gels were not covered with a realistic basal lamina, and the passive barrier function of the basal lamina laid down by the endothelial cells needs to be investigated further. However, endothelial cells adhered well to the gels and formed a confluent monolayer within 24 h. Second, the macrovascular HUVECs used in this assay differ from microvascular endothelial cells with respect to their adhesion molecule expression levels and chemokine secretion (21,39). Such differences, however, have been reported to be no greater than those seen between microvascular endothelial cells from different organs (21,40).

We tested the transmigration and invasion behavior of 11 tumor cells cultured on HPMECs and could largely replicate the findings obtained on HUVECs, but with one notable exception: A431 lung carcinoma cells that remain noninvasive on HUVECs became clearly invasive when cultured on HPMECs (Fig. 2). This finding suggests that endothelial cells from different organs differ in their barrier function against specific tumor cell types and thereby guide these tumor cells to metastasize preferentially in different organs (41). However, given the large diversity of tumor cell lines tested in this study, any arbitrary choice of an organ-specific microvascular endothelial cell would unnecessarily complicate

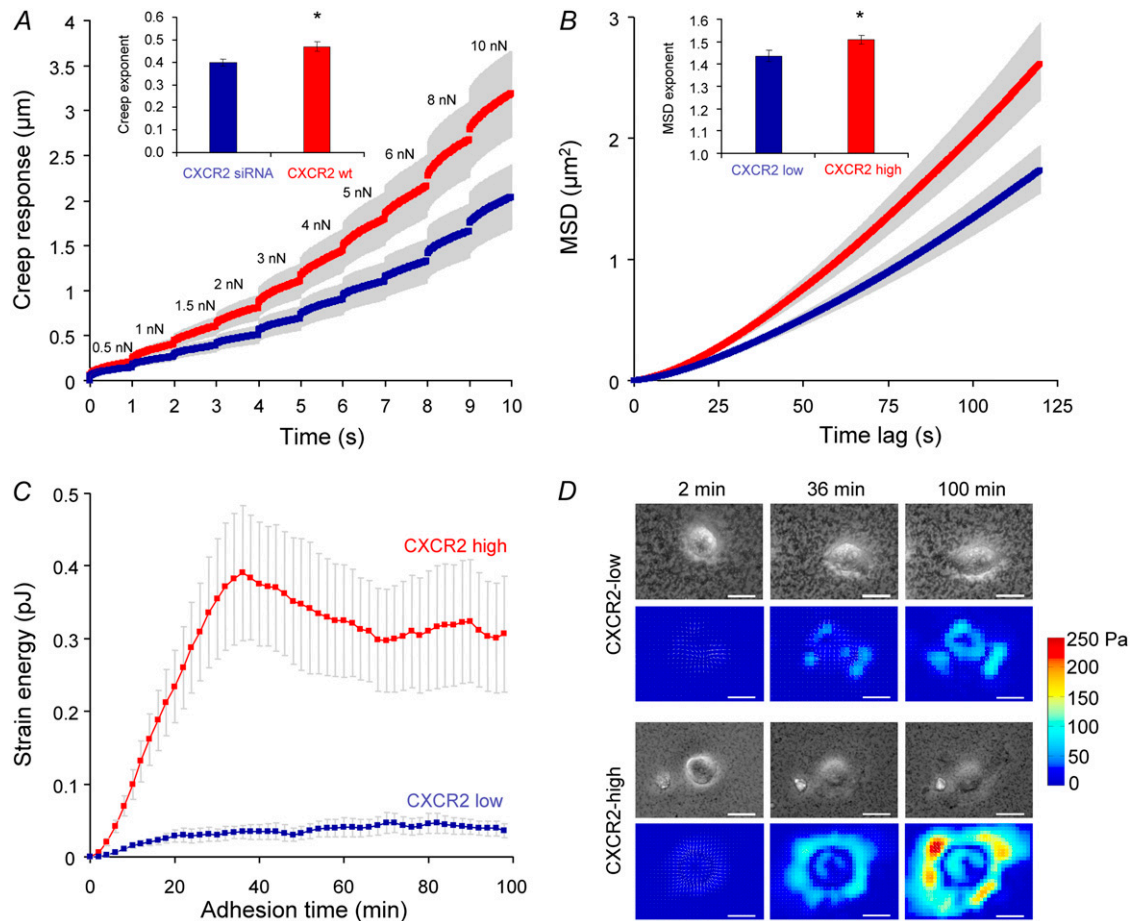


FIGURE 7 CXCR2 expression modulates cell mechanics, cytoskeletal dynamics, and tractions in MDA-MB-231 breast carcinoma cells. (A) Assay 1: The displacements of integrin-bound magnetic beads to step forces between 0.5 and 10 nN (creep response) followed a superposition of power laws in time with exponents that were significantly higher in CXCR2 wild-type cells compared with CXCR2 knockdown cells (see *inset*, $p < 0.05$). (B) Assay 2: Mean square displacement (MSD) of unforced beads attached to CXCR2-high cells revealed a more superdiffusive behavior (see *inset*, $p < 0.05$). (C) Assay 3: Elastic strain energy generated by CXCR2-high cells during adhesion on a polyacrylamide gel was eightfold higher than that by CXCR2-low cells. (D) Example of a traction map beneath a CXCR2-low cell (*top*) and a CXCR2-high cell (*bottom*) after 2, 36, and 100 min of adhesion time. Maximum tractions were substantially higher in CXCR2-high cells. Scale bars are 20 μm .

the transmigration assay for reasons of limited supply, reduced proliferation, and longer culture time, poorer monolayer formation, need for increased serum and growth factor concentrations in the culture medium, and the need to use cells in higher passages. For our experiments, especially for the formation of a closed monolayer, it was crucial that HUVECs were freshly isolated for each experiment and that they were not previously frozen and were unpassaged.

The most important finding of our study is that the endothelium formed a barrier only against 9 of 24 invasive cell lines. Unexpectedly, in six other cell lines, the endothelium substantially increased tumor cell invasion. Previous studies have reported only a barrier function but not an enhancing function (16). Moreover, 11 cell lines that were noninvasive in the absence of an endothelium became invasive in its presence (Table 1). These data support the hypothesis that the endothelium may act as a key modulator for metastasis for-

mation (9,15,16). We also showed that single or clustered microvascular endothelial cells that were co-plated at the same time with MDA-MB-231 tumor cell increased invasiveness, but interestingly, invasiveness increased even more when an endothelial cell monolayer had already formed before the addition of tumor cells (Fig. 2, *inset*). This raises the question of the mechanism by which the endothelium is able to selectively modulate tumor cell transmigration.

The degree of tumor cell invasiveness in the absence or presence of endothelial cells did not depend on the tissue type from which the tumor cells were derived (Table 1). In contrast to several reports, we found that none of the invasive tumor cells destroyed or disrupted the endothelial monolayer or induced apoptosis in endothelial cells (7,16,42) (Fig. 1). Microarray analysis revealed that endothelial cells altered their gene expression when they were cocultured with tumor cells (Fig. 3). The regulation of some of the endothelial cell

genes depended on the ability of the tumor cells to transmigrate through the endothelium (Fig. 3). Endothelial cell genes that were upregulated in the presence of invasive tumor cells included cytoskeletal proteins, cell-cell adhesion molecules, and the CXC chemokines Gro- β , IL-8, and I-TAC. This study focused on chemokines and their receptors as modulators for the interaction between tumor cells and endothelial cells.

As expected from the microarray data (Fig. 3), the addition of exogenous Gro- β and IL-8 significantly increased tumor cell transmigration and invasion. Gro- α , Gro- β , and Gro- γ all bind to the same CXCR2 chemokine receptor and have been reported to enhance melanoma tumor growth (43–45). IL-8 also binds to the CXCR2 chemokine receptor and reportedly increases invasiveness of PC-3 prostate carcinoma cells (22). FACS analysis of all 51 tumor cell lines revealed that invasive tumor cells expressed significantly more CXCR2 than noninvasive tumor cells (Fig. 5). This is consistent with previous studies that have shown that malignant PC-3 prostate carcinoma cells and prostate tumors at an advanced disease stage express increased levels of CXCR2 (22,46,47).

Interactions between the CXCR2 receptor on endothelial cells and CXCR2 ligand secretion by tumor cells have been reported to increase metastasis formation by enhancing angiogenesis (45,48). However, the HUVECs and HPMECs used in our experiments did not express detectable amounts of CXCR2 (Fig. 4). Therefore, in contrast to the previously identified interaction pathway, we attribute the increased tumor cell transmigration and invasion to an increased CXCR2 expression on tumor cells that are being stimulated by increased concentrations of Gro- β and IL-8 produced by endothelial cells. Other chemokines and their receptors, including the I-TAC receptor CXCR3, as well as the MCP-1 receptor CCR2, were expressed in noninvasive and invasive tumor cells at similar levels (Fig. 4). This is consistent with our finding that exogenous I-TAC and MCP-1 chemokines did not enhance tumor cell invasion, and indeed, I-TAC even reduced tumor cell invasion in the absence of an endothelium (Fig. 3). Of all the tumor cells tested, only the interactions between CXCR2 and its chemokine ligands were conspicuous and provide, therefore, a common mechanism for enhancing tumor cell invasion in the presence of endothelial cells.

To further analyze the function of the CXCR2 chemokine receptor, variants of MDA-MB-231, 786-O, and DU145 carcinoma cells were established that expressed high and low levels of CXCR2 (Fig. 5). In the absence of an endothelial monolayer, the invasion of CXCR2 high-expressing carcinoma cells was only slightly increased, but in the presence of an endothelial monolayer, the invasion was strongly increased (Fig. 5). MDA-MB-231 cells treated with the CXCR2 inhibitor SB225002 showed nearly complete inhibition of any invasion (Fig. S2). When CXCR2 was knocked down in MDA-MB-231 cells by siRNA, the presence of an endothelial cell layer failed to enhance tumor cell invasiveness (Fig. 6).

CXC receptor-ligand interactions are known to initiate a large number of signal transduction pathways involving activation of Rho, Rac, Cdc42, Erk, Akt, phospholipase C, and inositol-1,4,5-trisphosphate (49,50). This raises the question of possible downstream effects of pathways that may contribute to a more invasive and motile behavior of tumor cells. Recent studies have shown that the invasion speed of tumor cells through a three-dimensional matrix is governed by a dynamic equilibrium among traction forces, adhesion forces, and matrix deformation forces (37). In this work, the dynamics and stability of the force transfer between adhesion receptors and the cytoskeleton were investigated by analyzing the motion of magnetically forced and unforced fibronectin-coated microbeads. The beads were attached to integrin receptors of tumor cell variants that expressed low and high amounts of CXCR2 chemokine receptors (51). Beads on the cells with high CXCR2 expression displayed behavior that was indicative of an increased rate of adhesion/de-adhesion and cytoskeletal remodeling events, both of which promote cell invasion (37) (Fig. 7, A and B). At the same time, high-CXCR2 cells generated substantially higher contractile and adhesive forces and hence should be able to propel themselves more forcefully through an extracellular matrix (Fig. 7, C and D).

In summary, we found that, in the presence of invasive tumor cells, Gro- β and IL-8 chemokines were upregulated in endothelial cells and that CXCR2 receptors were highly expressed on invasive tumor cells, regardless of the tissue origin of the tumor. The interactions between CXCR2 and Gro- β or IL-8 lead to higher tractions and enhanced dynamics of cytoskeletal remodeling processes in tumor cells and represent a generic mechanism for the breakdown of the endothelial barrier function against tumor cell invasion.

SUPPLEMENTARY MATERIAL

To view all of the supplemental files associated with this article, visit www.biophysj.org.

We thank Ludger Klein-Hitpass for help with the microarray analysis, Peter Altevogt for the kind gift of A125 and KS cells, Barbara Reischl for excellent technical assistance, Robert Schmiedl for help with scanning EM imaging, Julia Resch and Joachim Kaschta for rheology measurements of collagen gels, and Wolfgang H. Goldmann for critical comments. This work was supported by Deutsche Krebshilfe (107384), DFG (MA 534/20-4), and NIH (HL65960).

REFERENCES

1. Liotta, L. A., P. S. Steeg, and W. G. Stetler-Stevenson. 1991. Cancer metastasis and angiogenesis: an imbalance of positive and negative regulation. *Cell*. 64:327–336.
2. Langley, R. R., and I. J. Fidler. 2007. Tumor cell-organ microenvironment interactions in the pathogenesis of cancer metastasis. *Endocr. Rev.* 28:297–321.
3. Steeg, P. S. 2006. Tumor metastasis: mechanistic insights and clinical challenges. *Nat. Med.* 12:895–904.

4. Nicolson, G. L. 1989. Metastatic tumor cell interactions with endothelium, basement membrane and tissue. *Curr. Opin. Cell Biol.* 1:1009–1019.
5. Stetler-Stevenson, W. G., S. Aznavoorian, and L. A. Liotta. 1993. Tumor cell interactions with the extracellular matrix during invasion and metastasis. *Annu. Rev. Cell Biol.* 9:541–573.
6. Luzzi, K. J., I. C. MacDonald, E. E. Schmidt, N. Kerkvliet, V. L. Morris, A. F. Chambers, and A. C. Groom. 1998. Multistep nature of metastatic inefficiency: dormancy of solitary cells after successful extravasation and limited survival of early micrometastases. *Am. J. Pathol.* 153:865–873.
7. Weis, S., J. Cui, L. Barnes, and D. Cheresh. 2004. Endothelial barrier disruption by VEGF-mediated Src activity potentiates tumor cell extravasation and metastasis. *J. Cell Biol.* 167:223–229.
8. Voura, E. B., R. A. Ramjessingh, A. M. Montgomery, and C. H. Siu. 2001. Involvement of integrin alpha(v)beta(3) and cell adhesion molecule L1 in transendothelial migration of melanoma cells. *Mol. Biol. Cell.* 12:2699–2710.
9. Tremblay, P. L., F. A. Auger, and J. Huot. 2006. Regulation of transendothelial migration of colon cancer cells by E-selectin-mediated activation of p38 and ERK MAP kinases. *Oncogene.* 25:6563–6573.
10. Sandig, M., E. B. Voura, V. I. Kalnins, and C. H. Siu. 1997. Role of cadherins in the transendothelial migration of melanoma cells in culture. *Cell Motil. Cytoskeleton.* 38:351–364.
11. Fidler, I. J., and I. R. Hart. 1982. Biological diversity in metastatic neoplasms: origins and implications. *Science.* 217:998–1003.
12. Al-Mehdi, A. B., K. Tozawa, A. B. Fisher, L. Shientag, A. Lee, and R. J. Muschel. 2000. Intravascular origin of metastasis from the proliferation of endothelium-attached tumor cells: a new model for metastasis. *Nat. Med.* 6:100–102.
13. Laferriere, J., F. Houle, M. M. Taher, K. Valerie, and J. Huot. 2001. Transendothelial migration of colon carcinoma cells requires expression of E-selectin by endothelial cells and activation of stress-activated protein kinase-2 (SAPK2/p38) in the tumor cells. *J. Biol. Chem.* 276:33762–33772.
14. Rousseau, S., F. Houle, J. Landry, and J. Huot. 1997. p38 MAP kinase activation by vascular endothelial growth factor mediates actin reorganization and cell migration in human endothelial cells. *Oncogene.* 15:2169–2177.
15. Li, Y. H., and C. Zhu. 1999. A modified Boyden chamber assay for tumor cell transendothelial migration in vitro. *Clin. Exp. Metastasis.* 17:423–429.
16. Heyder, C., E. Gloria-Maercker, F. Entschladen, W. Hatzmann, B. Niggemann, K. S. Zanker, and T. Dittmar. 2002. Realtime visualization of tumor cell/endothelial cell interactions during transmigration across the endothelial barrier. *J. Cancer Res. Clin. Oncol.* 128:533–538.
17. Wittchen, E. S., R. A. Worthylake, P. Kelly, P. J. Casey, L. A. Quilliam, and K. Burridge. 2005. Rap1 GTPase inhibits leukocyte transmigration by promoting endothelial barrier function. *J. Biol. Chem.* 280:11675–11682.
18. Chandrasekharan, U. M., M. Siemionow, M. Unsal, L. Yang, E. Poptic, J. Bohn, K. Ozer, Z. Zhou, P. H. Howe, M. Penn, and P. E. DiCorleto. 2006. TNF- α receptor-II is required for TNF- α -induced leukocyte-endothelial interaction in vivo. *Blood.*
19. McGettrick, H. M., J. M. Lord, K. Q. Wang, G. E. Rainger, C. D. Buckley, and G. B. Nash. 2006. Chemokine- and adhesion-dependent survival of neutrophils after transmigration through cytokine-stimulated endothelium. *J. Leukoc. Biol.* 79:779–788.
20. Gallatin, W. M., I. L. Weissman, and E. C. Butcher. 1983. A cell-surface molecule involved in organ-specific homing of lymphocytes. *Nature.* 304:30–34.
21. Hillyer, P., E. Mordelet, G. Flynn, and D. Male. 2003. Chemokines, chemokine receptors and adhesion molecules on different human endothelia: discriminating the tissue-specific functions that affect leukocyte migration. *Clin. Exp. Immunol.* 134:431–441.
22. Reiland, J., L. T. Furcht, and J. B. McCarthy. 1999. CXC-chemokines stimulate invasion and chemotaxis in prostate carcinoma cells through the CXCR2 receptor. *Prostate.* 41:78–88.
23. Mierke, C. T., M. Ballmaier, U. Werner, M. P. Manns, K. Welte, and S. C. Bischoff. 2000. Human endothelial cells regulate survival and proliferation of human mast cells. *J. Exp. Med.* 192:801–811.
24. Thomas, H., S. Senkel, S. Erdmann, T. Arndt, G. Turan, L. Klein-Hitpass, and G. U. Ryffel. 2004. Pattern of genes influenced by conditional expression of the transcription factors HNF6, HNF4alpha and HNF1beta in a pancreatic beta-cell line. *Nucleic Acids Res.* 32:e150.
25. Alenghat, F. J., B. Fabry, K. Y. Tsai, W. H. Goldmann, and D. E. Ingber. 2000. Analysis of cell mechanics in single vinculin-deficient cells using a magnetic tweezer. *Biochem. Biophys. Res. Commun.* 277:93–99.
26. Mierke, C. T., P. Kollmannsberger, D. Paranhos-Zitterbart, J. Smith, B. Fabry, and W. H. Goldmann. 2008. Mechano-coupling and regulation of contractility by the vinculin tail domain. *Biophys. J.* 94:661–670.
27. Fabry, B., G. N. Maksym, J. P. Butler, M. Glogauer, D. Navajas, and J. J. Fredberg. 2001. Scaling the microrheology of living cells. *Phys. Rev. Lett.* 87:148102.
28. Hildebrandt, J. 1969. Comparison of mathematical models for cat lung and viscoelastic balloon derived by Laplace transform methods from pressure-volume data. *Bull. Math. Biophys.* 31:651–667.
29. Bursac, P., G. Lenormand, B. Fabry, M. Oliver, D. A. Weitz, V. Viasnoff, J. P. Butler, and J. J. Fredberg. 2005. Cytoskeletal remodeling and slow dynamics in the living cell. *Nat. Mater.* 4:557–561.
30. Raupach, C., D. P. Zitterbart, C. T. Mierke, C. Metzner, F. A. Muller, and B. Fabry. 2007. Stress fluctuations and motion of cytoskeletal-bound markers. *Phys. Rev. E Stat. Nonlin. Soft Matter Phys.* 76:011918.
31. Butler, J. P., I. M. Tolic-Norrelykke, B. Fabry, and J. J. Fredberg. 2002. Traction fields, moments, and strain energy that cells exert on their surroundings. *Am. J. Physiol. Cell Physiol.* 282:C595–C605.
32. Lu, Y., Z. Cai, D. L. Galson, G. Xiao, Y. Liu, D. E. George, M. F. Melhem, Z. Yao, and J. Zhang. 2006. Monocyte chemotactic protein-1 (MCP-1) acts as a paracrine and autocrine factor for prostate cancer growth and invasion. *Prostate.* 66:1311–1318.
33. Youngs, S. J., S. A. Ali, D. D. Taub, and R. C. Rees. 1997. Chemokines induce migrational responses in human breast carcinoma cell lines. *Int. J. Cancer.* 71:257–266.
34. Muller, A., B. Homey, H. Soto, N. Ge, D. Catron, M. E. Buchanan, T. McClanahan, E. Murphy, W. Yuan, S. N. Wagner, J. L. Barrera, A. Mohar, E. Verastegui, and A. Zlotnik. 2001. Involvement of chemokine receptors in breast cancer metastasis. *Nature.* 410:50–56.
35. Salcedo, R., J. H. Resau, D. Halverson, E. A. Hudson, M. Dambach, D. Powell, K. Wasserman, and J. J. Oppenheim. 2000. Differential expression and responsiveness of chemokine receptors (CXCR1–3) by human microvascular endothelial cells and umbilical vein endothelial cells. *FASEB J.* 14:2055–2064.
36. Murdoch, C., P. N. Monk, and A. Finn. 1999. CXC chemokine receptor expression on human endothelial cells. *Cytokine.* 11:704–712.
37. Zaman, M. H., L. M. Trapani, A. Siemeski, D. Mackellar, H. Gong, R. D. Kamm, A. Wells, D. A. Lauffenburger, and P. Matsudaira. 2006. Migration of tumor cells in 3D matrices is governed by matrix stiffness along with cell-matrix adhesion and proteolysis. *Proc. Natl. Acad. Sci. USA.* 103:10889–10894.
38. Lin, Y., R. Huang, L. Chen, S. Li, Q. Shi, C. Jordan, and R. P. Huang. 2004. Identification of interleukin-8 as estrogen receptor-regulated factor involved in breast cancer invasion and angiogenesis by protein arrays. *Int. J. Cancer.* 109:507–515.
39. Aird, W. C. 2007. Phenotypic heterogeneity of the endothelium: I. Structure, function, and mechanisms. *Circ. Res.* 100:158–173.
40. Aird, W. C. 2007. Phenotypic heterogeneity of the endothelium: II. Representative vascular beds. *Circ. Res.* 100:174–190.
41. Ruoslahti, E. 2004. Vascular zip codes in angiogenesis and metastasis. *Biochem. Soc. Trans.* 32:397–402.
42. Li, A., M. L. Varney, and R. K. Singh. 2001. Expression of interleukin 8 and its receptors in human colon carcinoma cells with different metastatic potentials. *Clin. Cancer Res.* 7:3298–3304.

43. Owen, J. D., R. Strieter, M. Burdick, H. Haghnegahdar, L. Nanney, R. Shattuck-Brandt, and A. Richmond. 1997. Enhanced tumor-forming capacity for immortalized melanocytes expressing melanoma growth stimulatory activity/growth-regulated cytokine beta and gamma proteins. *Int. J. Cancer*. 73:94–103.
44. Haghnegahdar, H., J. Du, D. Wang, R. M. Strieter, M. D. Burdick, L. B. Nanney, N. Cardwell, J. Luan, R. Shattuck-Brandt, and A. Richmond. 2000. The tumorigenic and angiogenic effects of MGSA/GRO proteins in melanoma. *J. Leukoc. Biol.* 67:53–62.
45. Loukinova, E., G. Dong, I. Enamorado-Ayalya, G. R. Thomas, Z. Chen, H. Schreiber, and C. Van Waes. 2000. Growth regulated oncogene-alpha expression by murine squamous cell carcinoma promotes tumor growth, metastasis, leukocyte infiltration and angiogenesis by a host CXC receptor-2 dependent mechanism. *Oncogene*. 19:3477–3486.
46. Varney, M. L., A. Li, B. J. Dave, C. D. Bucana, S. L. Johansson, and R. K. Singh. 2003. Expression of CXCR1 and CXCR2 receptors in malignant melanoma with different metastatic potential and their role in interleukin-8 (CXCL-8)-mediated modulation of metastatic phenotype. *Clin. Exp. Metastasis*. 20:723–731.
47. Murphy, C., M. McGurk, J. Pettigrew, A. Santinelli, R. Mazzucchelli, P. G. Johnston, R. Montironi, and D. J. Waugh. 2005. Nonapical and cytoplasmic expression of interleukin-8, CXCR1, and CXCR2 correlates with cell proliferation and microvessel density in prostate cancer. *Clin. Cancer Res.* 11:4117–4127.
48. Mestas, J., M. D. Burdick, K. Reckamp, A. Pantuck, R. A. Figlin, and R. M. Strieter. 2005. The role of CXCR2/CXCR2 ligand biological axis in renal cell carcinoma. *J. Immunol.* 175:5351–5357.
49. Schraufstatter, I. U., J. Chung, and M. Burger. 2001. IL-8 activates endothelial cell CXCR1 and CXCR2 through Rho and Rac signaling pathways. *Am. J. Physiol. Lung Cell. Mol. Physiol.* 280:L1094–L1103.
50. Venkatakrishnan, G., R. Salgia, and J. E. Groopman. 2000. Chemokine receptors CXCR-1/2 activate mitogen-activated protein kinase via the epidermal growth factor receptor in ovarian cancer cells. *J. Biol. Chem.* 275:6868–6875.
51. Choquet, D., D. P. Felsenfeld, and M. P. Sheetz. 1997. Extracellular matrix rigidity causes strengthening of integrin- cytoskeleton linkages. *Cell*. 88:39–48.